Carcinogenesis vol.31 no.8 pp.1329–1337, 2010
doi:10.1093/carcin/bgq083
Advance Access publication May 14, 2010

Downregulation of *Fzd6* and *Cthrc1* and upregulation of olfactory receptors and protocadherins by dietary beta-carotene in lungs of *Bcmo1*$^{-/-}$ mice

Yvonne G.J.van Helden[1,2,3], Roger W.Godschalk[2], Sandra G.Heil[1,3], Annelies Bunschoten[1], Susanne Hessel[4], Jaume Amengual[5,6], M.Luisa Bonet[5], Johannes von Lintig[6], Frederik J.van Schooten[2] and Jaap Keijer[1,*]

[1]Human and Animal Physiology, Wageningen University, PO Box 338, 6700 AH Wageningen, The Netherlands, [2]Department of Health Risk Analysis and Toxicology, Research Institute NUTRIM, Maastricht University, Maastricht 6200 MD, The Netherlands, [3]RIKILT-Institute of Food Safety, Wageningen 6700 AE, The Netherlands, [4]Institute of Biology I, Freiburg D-79104, Germany, [5]Laboratory of Molecular Biology, Nutrition and Biotechnology, University of the Balearic Islands and CIBER de Fisiopatología de la Obesidad y Nutrición, Palma de Mallorca, Spain and [6]Department of Pharmacology, School of Medicine, Case Western Reserve University, Cleveland 44106-4965, OH, USA

*To whom correspondence should be addressed. Tel: +31 317 484 136; Fax: +31 317 484 077;
Email: jaap.keijer@wur.nl

An ongoing controversy exists on beneficial versus harmful effects of high beta-carotene (BC) intake, especially for the lung. To elucidate potential mechanisms, we studied effects of BC on lung gene expression. We used a *beta-carotene 15,15′-monooxygenase 1* (*Bcmo1*) knockout mouse (*Bcmo1*$^{-/-}$) model, unable to convert BC to retinoids, and wild-type mice (*Bcmo1*$^{+/+}$) mice to dissect the effects of intact BC from effects of BC metabolites. As expected, BC supplementation resulted in a higher BC accumulation in lungs of *Bcmo1*$^{-/-}$ mice than in lungs of *Bcmo1*$^{+/+}$ mice. Whole mouse genome transcriptome analysis on lung tissue revealed that more genes were regulated in *Bcmo1*$^{-/-}$ mice than *Bcmo1*$^{+/+}$ mice upon BC supplementation. *Frizzled homolog 6* (*Fzd6*) and *collagen triple helix repeat containing 1* (*Cthrc1*) were significantly downregulated (fold changes −2.99 and −2.60, respectively, false discovery rate < 0.05) by BC in *Bcmo1*$^{-/-}$. Moreover, many olfactory receptors and many members of the protocadherin family were upregulated. Since both olfactory receptors and protocadherins have an important function in sensory nerves and *Fzd6* and *Cthrc1* are important in stem cell development, we hypothesize that BC might have an effect on the highly innervated pulmonary neuroendocrine cell (PNEC) cluster. PNECs are highly associated with sensory nerves and are important cells in the control of stem cells. A role for BC in the innervated PNEC cluster might be of particular importance in smoke-induced carcinogenesis since PNEC-derived lung cancer is highly associated with tobacco smoke.

Introduction

Beta-carotene (BC) is an orange colored phytochemical present in dark green vegetables and colored fruits and is widely used as a coloring agent. BC can be metabolized into vitamin A and is used in supplements to correct for vitamin A deficiency. BC is considered to be a health-promoting agent because of its antioxidant properties, thereby preventing radical-induced macromolecular damage. Indeed, many epidemiological studies showed that an increased intake of dietary BC, as well as increased BC plasma concentration, is associated with a decreased risk for cardiovascular diseases and several types of cancer, including lung cancer (1,2). Because of this, two large-scale human intervention trials were performed with the intention to decrease lung cancer risk by BC supplementation in male smokers [Alpha-Tocopherol, Beta-Carotene cancer prevention study (ATBC)] and in male and female smokers or asbestos-exposed subjects [carotene and retinol efficacy trial (CARET)]. Unexpectedly, both studies showed an increased lung cancer risk upon BC supplementation compared with placebo-supplemented subjects (3,4). At the same time, a study performed mainly in non-smokers showed no effect of BC on lung cancer risk (5). Together, studies indicate that BC has health-promoting capacities, but high intakes can also result in adverse health effects such as an increased lung cancer risk in smokers and asbestos-exposed subjects. The underlying mechanisms for the adverse effects of BC action are not precisely known, although several mechanisms have been suggested, e.g. BC or BC metabolites can become pro-oxidants at high concentrations (6) or in combination with oxidative stress (7). There is also evidence that BC supplementation can result in different levels of the bioactive BC metabolites such as retinoic acid, which is able to bind to retinoic acid receptors (RARs) and retinoid X receptors (RXRs) to activate these transcription factors. Additionally, retinoic acid-induced catabolism can decrease RAR and RXR activity, thereby specifically increasing cell proliferation (8). However, the exact mechanism is unknown mainly because BC metabolism greatly differs between humans and mammalian model organisms such as mice.

In humans, an increased intake of BC results in an increase in plasma concentrations of BC and its metabolites. Beta-carotene 15,15′-monooxygenase 1 (Bcmo1) is a key enzyme in BC metabolism that cleaves BC symmetrically to form two molecules of retinal, which can be further metabolized into several other downstream BC metabolites (9). Rodents, which are herbivores and therefore depend on the production of vitamin A from pro-vitamin A carotenoids such as BC, possess a more active Bcmo1 variant than man. Although in humans, a significant portion of BC is found intact in plasma, rodents cleave virtually all absorbed BC to facilitate their vitamin A requirements (10).

The aim of our study was to investigate BC-induced gene expression changes in the lung. Therefore, male *Bcmo1*$^{+/+}$ mice and *Bcmo1*$^{-/-}$ mice were fed for 14 weeks with a vitamin A sufficient diet (1500 IU/kg) without (control) or with supplementation of BC (BC, 150 mg/kg diet) and microarray analysis was performed (mouse whole genome arrays) on lung complementary RNA (cRNA). We were mainly interested in effects of BC in the *Bcmo1*$^{-/-}$ mice since BC is able to accumulate in tissues of these mice (11). To dissociate effects induced by BC from effects induced by BC metabolites, *Bcmo1*$^{+/+}$ mice were taken along.

Abbreviations: BC, beta-carotene; *Bcmo1*, *beta-carotene 15,15′-monooxygenase 1*; *Cthrc1*, *collagen triple helix repeat containing 1*; cDNA, complementary DNA; CARET, carotene and retinol efficacy trial; cRNA, complementary RNA; Cy3, cyanine 3-cytidine triphosphate; Cy5, cyanine 5-cytidine triphosphate; FDR, false discovery rate; *Fzd6*, *frizzled homolog 6*; GO, Gene Ontology; HPLC, high-performance liquid chromatography; *Olfr*, *olfactory receptor*; PNEC, pulmonary neuroendocrine cell; Q-PCR, real-time quantitative polymerase chain reaction; RAR, retinoic acid receptor; RXR, retinoid X receptor; SOM, self-organizing map.

Materials and methods

Animals and treatment

Twelve male B6129SF1 (*Bcmo1*$^{+/+}$) and twelve male B6;129S-*Bcmo1*^{tm1dnp} (*Bcmo1*$^{-/-}$) mice, described previously by Hessel *et al.* (11) were used for the experiment. The mouse experiment was conducted in accordance with the German animal protection laws by the guidelines of the local veterinary authorities. During the breeding and weaning periods of the mice, dams were maintained on KLIBA 3430 chow diet containing 14000 IU vitamin A/kg (Provima Kliba AG, Kaiseraugst, Switzerland). Five-week-old *Bcmo1*$^{+/+}$ and *Bcmo1*$^{-/-}$ mice were caged in groups containing two to three siblings per group and were maintained under environmentally controlled conditions (temperature 24°C, 12 h/12 h light/dark cycle). Mice had *ad libitum* access to feed and water. Basic feed consisted of the palletized diet D12450B (Research Diets, Inc., New Brunswick, NJ) with a fat content of 10%. The diet was modified to contain 1500 IU vitamin A/kg of diet, which is a vitamin A

sufficient diet, and the control diet (control) was supplemented with water soluble vehicle beadlets (DSM Nutritional Products Ltd, Basel, Switzerland) containing DL-alpha-tocopherol and ascorbyl palmitate as stabilizers, as well as carriers such as gelatine, corn oil sucrose and starch. The BC diet (BC) was supplemented with identical water-soluble beadlets containing BC (DSM Nutritional Products Ltd) to generate 150 mg BC/kg diet. Beadlets were added by the manufacturer before low temperature pelletting. Feed pellets were color marked and stored at 4°C in the dark. After 14 weeks of dietary intervention, six *Bcmo1*$^{+/+}$ mice on the control diet (*Bcmo1*$^{+/+}$ Co), six *Bcmo1*$^{+/+}$ mice on the BC diet (*Bcmo1*$^{+/+}$ BC), six *Bcmo1*$^{-/-}$ on the control diet (*Bcmo1*$^{-/-}$ Co) and six *Bcmo1*$^{-/-}$ on the BC diet (*Bcmo1*$^{-/-}$ BC) were randomly killed during three subsequent mornings. Blood was collected from the vena cava after isoflurane and ketamine anesthesia. Blood was coagulated for at least 20 min at room temperature, cooled to 4°C and centrifuged. Lung tissue was removed, rinsed in phosphate buffered saline and snap frozen in liquid nitrogen. The lung tissues were stored at −80°C.

High-performance liquid chromatography separation of retinoids and carotenoids

Retinoids and carotenoids were extracted from lung tissues and plasma under dim red safety light ($\lambda \geq 600$ nm). Briefly, tissues (20–40 mg) were homogenized in 200 µl of 2 M hydroxylamine (pH 6.8) and 200 µl of methanol with a glass homogenizer. For determination of BC and retinol in serum, 180 µl serum was added to 200 µl methanol. Then 400 µl acetone was added either to these plasma or tissue extracts. Extraction of carotenoids and retinoids was performed with petroleum ether. The extraction was repeated three times, and the collected organic phases were dried under nitrogen and dissolved in high-performance liquid chromatography (HPLC) solvent (*n*-hexane:ethanol, 99.5:0.5). HPLC separation of BC and retinoids and quantification of peak integrals was performed as described previously (9). Solvents for HPLC and extraction were purchased in HPLC grade from Merck (Darmstadt, Germany).

Histology of the lung

Small pieces of upper right lung tissue of two randomly selected animals per group were fixed by immersion in 0.1 M sodium phosphate buffer containing 4% paraformaldehyde (pH 7.4) overnight at 4°C, thereafter dehydrated, cleared and then paraffin embedded. Three micrometers thick sections were cut and stained with Periodic Acid Schiff and Mayer's hematoxylin for histological analysis.

RNA isolation

Left lung lobes were homogenized in liquid nitrogen using a cooled mortar and pestle. Total RNA was isolated using TRIzol reagent (Invitrogen, Breda, The Netherlands) followed by purification using RNeasy columns (QIAGEN, Venlo, The Netherlands) using the instructions of the manufacturer. RNA concentration and purity were measured using the Nanodrop system (IsoGen Life Science, Maarssen, The Netherlands). Approximately 30 µg of total RNA was isolated with A_{260}:A_{280} ratios >2 and A_{260}:A_{230} ratios >1.9 for all samples, indicating good RNA purity. RNA degradation was checked on the Experion (Bio-Rad, Veenendaal, The Netherlands) using Experion StdSense chips (Bio-Rad).

Microarray hybridization procedure

The 4 × 44k Agilent whole mouse genome microarrays (G4122F; Agilent Technologies, Santa Clara, CA) were used. Preparation of the sample and the microarray hybridization were carried out according to the manufacturer's protocol with a few exceptions as described previously (12,13). In brief, complementary DNA (cDNA) was synthesized from 1 µg lung RNA using the Agilent Low RNA Input Fluorescent Linear Amplification Kit for each animal without addition of spikes. Thereafter, samples were split in two equal amounts, to synthesize cyanine 3-cytidine triphosphate (Cy3) and cyanine 5-cytidine triphosphate (Cy5) labeled cRNA using half the amounts per dye as indicated by the manufacturer (Agilent Technologies). Labeled cRNA was purified using RNeasy columns (QIAGEN). Yield, A_{260}/A_{280} ratio and Cy3 and Cy5 activity were examined for every sample using the nanodrop. All samples met the criteria of a cRNA yield higher than 825 ng and a specific activity of at least 8.0 pmol Cy3 and Cy5. Thousand two hundred nanograms of every Cy3-labeled cRNA sample was pooled and used as a common reference pool. Individual 825 ng Cy5-labeled cRNA and 825 ng pooled Cy3-labeled cRNA were fragmented in 1× fragmentation and 1× blocking agent (Agilent Technologies) at 60°C for 30 min and thereafter mixed with GEx Hybridization Buffer HI-RPM (Agilent Technologies) and hybridized in a 1:1 ratio at 65°C for 17 h in an Agilent Microarray hybridization Chamber rotating at 4 r.p.m. After hybridization, slides were washed according to the wash protocol with Stabilization and Drying solution (Agilent Technologies). Arrays were scanned with an Agilent scanner with 10% and 100% laser power intensities (Agilent Technologies).

Data analyses of microarray results

Signal intensities for each spot were quantified using Feature Extraction 9.1 (Agilent Technologies). Median density values and background values of each spot were extracted for both the experimental samples (Cy5) and the reference samples (Cy3). Quality control for every microarray was performed visually, by using Quality control graphs from Feature extraction and M-A plots and boxplots that were made using limmaGUI in R (Bioconductor) (14). Data were imported into GeneMaths XT 2.0 (Applied Maths, Sint-Martens-Latem, Belgium). Spots with a Cy5 and Cy3 signal twice above background were selected and log transformed. The Cy5 signal was normalized against the Cy3 intensity as described before (15). Supervised principal component analysis and self-organizing map (SOM) analysis were performed using GeneMaths XT. Direct biological interaction analysis was performed using Gene Ontology (GO) overrepresentation analysis (ErmineJ) (16) and literature data mining.

Analysis of messenger RNA expression by real-time quantitative polymerase chain reaction

Differential gene expression of *frizzled homolog 6* (*Fzd6*) and *collagen triple helix repeat containing 1* (*Cthrc1*) was analyzed using real-time quantitative polymerase chain reaction (Q-PCR) to validate microarray results. One microgram RNA isolated from lung of individual animals was converted into cDNA using the iScript cDNA Synthesis Kit (Bio-Rad). One sample was taken along without reverse transcriptase to examine the presence of DNA (-RT reaction). An equal amount of cDNA of all individual samples was pooled and diluted (10×, 31.6× 100×, 316× 1000×, 3160× and 10000×) for the generation of a calibration curve. Each polymerase chain reaction (25 µl) contained 1× iQ SYBR green supermix (Bio-Rad), 10 µM sense primer, 10 µM antisense primer and 2 µl 100 times diluted cDNA. Primers for *Fzd6* were sense 5′-ACTCCCAGCGCCAAAGATCG-3′ and antisense 5′-GCAGAGATGTGGAGCCCTTGAG-3′; for *Cthrc1*, sense 5′-TGGACCAAGGAAGCCCTGAGT-3′ and antisense 5′-TGAACAGGTGCCGACCCAGA-3; for *olfactory receptor 437* (*Olfr437*), sense 5′-TGGCCTGCGCCGACACTTTG and anti-sense 5′-GGCCTTCCTGCGACCCTCCT and for *protocadherin beta 9* (*Pcdhb9*), sense 5′-TGTTAGTGGATGGCTTCT and antisense 5′-ATGACCAGGTACAATGTAAG.

For the amplification of the reference genes, we used for *syntaxin 5a* (*Stx5a*), sense 5′-TTAAAGAACAGGAGGAAACGATTCAGAG-3′ and antisense 5′-CAGGCAAGGAAGACCACAAAGATG-3′ and for *ring finger protein 130* (*Rnf130*), sense 5′-ACAGGAACCAGCGTCGTCTTG-3′ and antisense 5′-ACCCGAACAACATCATTCTGCTTATAG-3′, which showed equal gene expression levels for all individual animals on the microarray. These intron-spanning primers were designed using Beacon designer 7.00 (Premier Biosoft International, Palo Alto, CA) or using primer-BLAST (*Cthrc1*) (http://www.ncbi.nlm.nih.gov/). Amplification was performed in duplicate for *Fzd6* and *Cthrc1* and in quadruplets for *Olfr437* and *Pcdhb9* because of the relatively low absolute expression levels and relatively low fold changes, using the MyIQ single-color real-time polymerase chain reaction detection system (Bio-Rad). We used the following temperature cycles: 1× 3 min at 95°C, 40× two-step amplification [15 s 95°C, 45 s 60°C (*Fzd6*, *Cthrc1*, *Stx5a* and *Rnf130*) or 54°C (*Olfr437*) or 57.5°C (*Pcdhb9*)], 1× 1 min 95°C and 1× 1 min 65°C followed by melting curve analysis (60× 10 s 65°C with an increase of 0.5°C per 10 s). A negative control without cDNA template and the -RT sample were taken along with every assay. Using the standard curves for every gene, the relative level of expression of all genes was calculated. Normalized Gene Expression ($\Delta\Delta C_T$) analysis for *Fzd6* and *Cthrc1* was calculated using the IQ5 software version 2.0 (Bio-Rad).

Statistical analysis

Fold changes for both microarray gene expression and Q-PCR gene expression were calculated using mean log signal intensities. *P*-values for differential expressions were calculated between two groups using Student's *t*-test statistics on log intensity values (Excel version 2003). Changes were considered statistically significant at $P < 0.05$. To identify 'marker-regulated genes' from other regulated genes, the Benjamini–Hochberg false discovery rate (FDR) testing method (Genemaths XT) was used to correct for multiple comparisons. The effects of Diet and Genotype on concentrations of BC, retinol and retinyl esters in lung and serum were analyzed using 2 × 2 factorial univariate analysis of variance (SPSS version 15.0) and considered statistically significant when $P < 0.05$. A Student's *t*-test was used to test for the effect of a BC diet versus control diet and considered statistically significant when $P < 0.05$. Correlations and differences in correlations between BC concentration and BC metabolite concentrations in lung were tested (SPSS) and considered significant when $P < 0.05$.

Results

BC metabolism in Bcmo1$^{+/+}$ mice and Bcmo1$^{-/-}$ mice

BC supplementation resulted in increased BC concentrations in serum and lung tissue. *Bcmo1*$^{-/-}$ mice accumulated ~3.5 times more BC in serum and ~2 times more BC in lung tissue than *Bcmo1*$^{+/+}$ mice upon BC supplementation. BC supplementation also resulted in an increased lung retinol and retinyl ester concentration in both *Bcmo1*$^{+/+}$ mice and *Bcmo1*$^{-/-}$ mice (Figure 1A–E). Correlations between concentrations of BC with retinol and BC with retinyl esters in mouse lung were made to investigate a possible dysregulation in BC metabolite accumulation. BC concentrations correlated significantly with retinol ($R = 0.705$, $P < 0.05$) and retinyl ester ($R = 0.90$, $P < 0.001$) concentrations in lungs of *Bcmo1*$^{+/+}$ mice. In *Bcmo1*$^{-/-}$, there was also a significant positive correlation between BC and retinol ($R = 0.74$, $P < 0.01$) or retinyl esters ($R = 0.89$, $P < 0.001$) in the lung. The slope of the correlation between BC and retinyl ester concentration in lungs of *Bcmo1*$^{-/-}$ compared with *Bcmo1*$^{+/+}$ mice were significantly different ($P < 0.001$), a similar difference in slopes was shown in the correlation between BC and retinol; this was however not significant (Figure 1F and G).

We also investigated whether gene expression differences were present in downstream BC metabolizing enzymes in *Bcmo1*$^{-/-}$ mice as compared with *Bcmo1*$^{+/+}$ mice and in BC-supplemented mice compared with control diet-fed mice. We found downregulation in gene expression of *alcohol dehydrogenase 7* (*class IV*), *mu or sigma polypeptide* (*Adh7*); upregulation in gene expression of *aldehyde dehydrogenase family 1*, *subfamily A2* (*Aldh1a2*); upregulation in gene expression of *aldehyde dehydrogenase 2*, *mitochondrial* (*Aldh2*) and an upregulation in gene expression of *lecithin-retinol acyltransferase* (*phosphatidylcholine-retinol-O-acyltransferase*) (*Lrat*) in *Bcmo1*$^{-/-}$ mice (Table I) as compared with *Bcmo1*$^{+/+}$ mice.

These data show that BC accumulation was present in BC-supplemented *Bcmo1*$^{-/-}$ mice. The tight correlation between retinyl esters and BC supplementation in both *Bcmo1*$^{+/+}$ mice was still tightly correlated in *Bcmo1*$^{-/-}$, although the ratio BC:retinyl esters was much higher in *Bcmo1*$^{-/-}$ mice. Moreover, the knockout of the

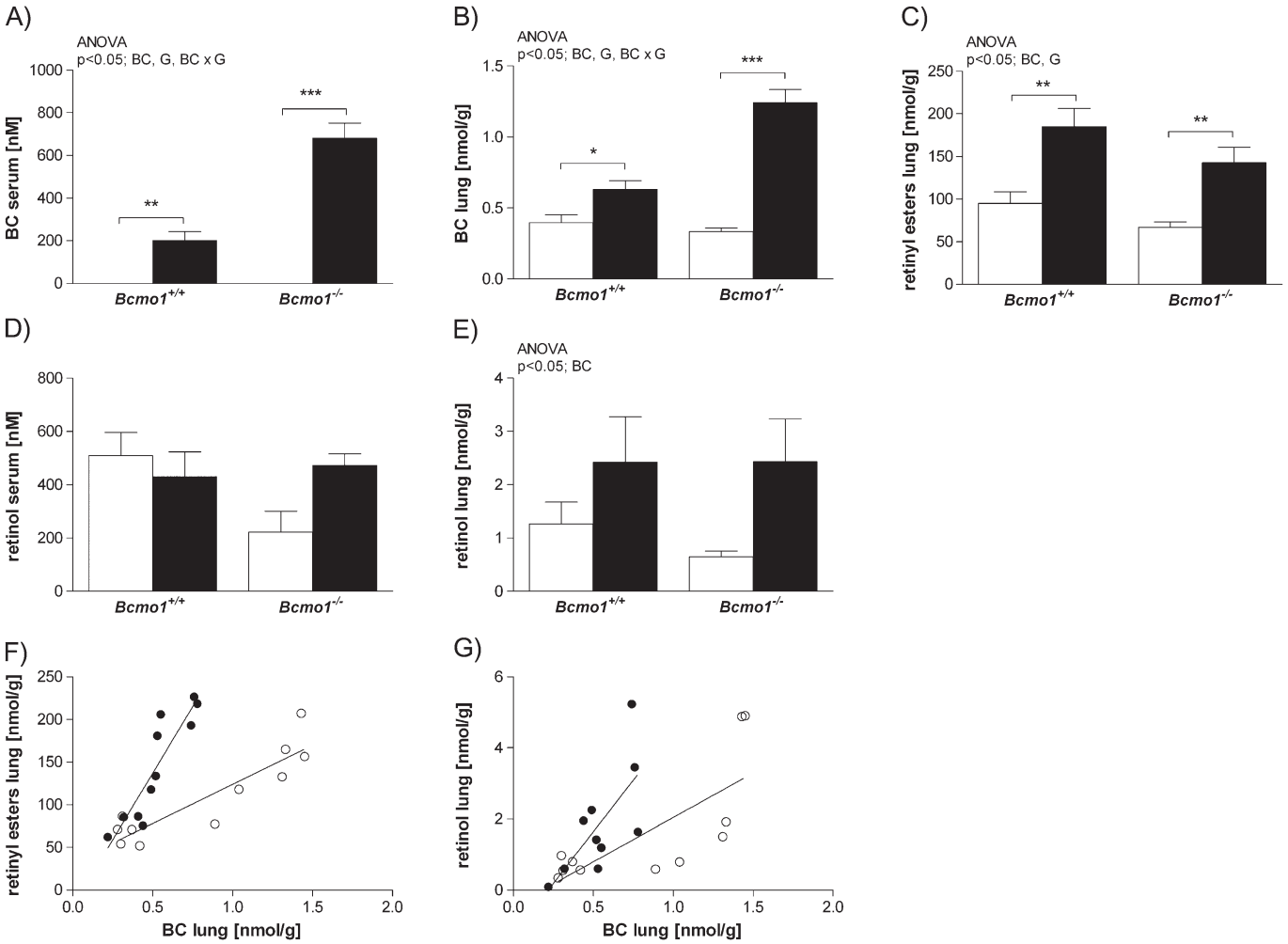

Fig. 1. BC and BC metabolite concentrations in lungs of *Bcmo1*$^{+/+}$ and *Bcmo1*$^{-/-}$ mice. BC concentration in serum (**A**) and lung tissue (**B**), retinyl ester concentration in lung tissue (**C**), retinol concentrations in serum (**D**) and in lung tissue (**E**) of male *Bcmo1*$^{+/+}$ mice and *Bcmo1*$^{-/-}$ mice fed a control diet (white bars) or a BC diet (black bars). Correlation of BC concentration and retinyl ester concentration in lung (**F**) (*Bcmo1*$^{+/+}$: $R = 0.90$, $P < 0.001$; *Bcmo1*$^{-/-}$: $R = 0.89$, $P < 0.001$) with significant different slopes ($P < 0.001$) for *Bcmo1*$^{+/+}$ (slope = 311.8) and *Bcmo1*$^{-/-}$ (91.94) and correlation of BC concentration and retinol concentration in lung (**G**) (*Bcmo1*$^{+/+}$: $R = 0.705$, $P < 0.05$; *Bcmo1*$^{-/-}$: $R = 0.746$, $P < 0.01$) with non-significant different slopes measured in *Bcmo1*$^{+/+}$ mice (closed circles) and *Bcmo1*$^{-/-}$ mice (open circles). Concentrations (A–E) are expressed as mean ± SEM, significance was tested for diet (BC) and genotype (G) using analysis of variance (ANOVA) and considered significant at $P < 0.05$. Significant effects for the different factors; diet (BC), genotype (G) or an interaction (BC × G) are displayed on top of each figure. A Student's *t*-test was used between BC and control groups when there was a significant diet effect using ANOVA and considered significant when $P < 0.05$. Using *t*-test statistics: $^{*}P < 0.05$, $^{**}P < 0.01$ and $^{***}P < 0.001$.

Table I. Genes involved in downstream BC metabolism and retinoic acid catabolism that were regulated by BC supplementation or knockout of *Bcmo1*

Gene symbol	Gene name	Sequence ID	Probe name	Gene expression*			
				Bcmo1$^{+/+}$		*Bcmo1*$^{-/-}$	
				Co	BC	Co	BC
Adh7	*alcohol dehydrogenase 7 (class IV), mu or sigma polyapeptide*	NM_009626	A_51_P233797	1.00^{a}	1.01^{a}	−1.83^{b}	−1.62^{b}
Aldh1a2	*aldehyde dehydrogenase family 1, subfamily A2*	NM_009022	A_52_P58145	1.00^{a}	−1.02^{a}	1.35^{b}	1.32^{b}
Aldh2	*aldehyde dehydrogenase 2, mitochondrial*	AK163452	A_52_P13109	1.00^{a}	−1.03^{a}	1.49^{b}	1.49^{b}
Lrat	*lecithin-retinol acyltransferase (phosphatidylcholine-retinol-O-acyltransferase)*	NM_023624	A_52_P669005	1.00^{a}	1.57^{b}	1.80^{bc}	2.67^{c}

*Gene expression relative to *Bcmo1*$^{+/+}$ control mice.
Different letters indicate a significant difference ($P < 0.05$).

important BC metabolizing enzyme *Bcmo1* resulted in a changed gene expression of other important downstream BC metabolizing enzymes.

BC supplementation downregulates Fzd6 and Cthrc1 gene expression in Bcmo1$^{-/-}$ *mice*

Histology did not show any obvious differences in lung structure between mice of the four different groups. We also analyzed gene expression changes in the lung of *Bcmo1*$^{+/+}$ mice and in *Bcmo1*$^{-/-}$ mice after feeding a BC diet. Supervised principal component analysis showed that mice were clearly separated based on genotype (principal component 1) and that *Bcmo1*$^{-/-}$ mice receiving the control diet were clearly separated from *Bcmo1*$^{-/-}$ mice receiving the BC-supplemented diet (principal component 2) (Figure 2A).

From the 43379 probe sets (number of spots without control spots) present on the array, 33414 spots had an intensity of more than twice above the background. Of these spots, 326 were differentially expressed ($P< 0.05$) in *Bcmo1*$^{+/+}$ mice (genes are listed in supplementary Table I, available at *Carcinogenesis* Online) and 1474 were differentially expressed ($P < 0.05$) in *Bcmo1*$^{-/-}$ mice (genes are listed in supplementary Table II, available at *Carcinogenesis* Online) upon BC supplementation (Figure 2B). Since BC accumulation was higher in *Bcmo1*$^{-/-}$ mice and more genes were significantly differentially expressed in *Bcmo1*$^{-/-}$ mice, we further focused on effects of BC in this group.

To identify key BC-regulated genes, FDR testing was performed. Two genes were downregulated by BC with a FDR < 0.05; *Fzd6*) and *Cthrc1* with a fold change of −2.99 and −2.60, respectively, in BC-supplemented *Bcmo1*$^{-/-}$ compared with *Bcmo1*$^{-/-}$ control mice. These genes had also the lowest *P*-values in the data set (Figure 2C). The significant downregulation of *Fzd6* and *Cthrc1* was confirmed by Q-PCR (Figure 3A and B). Nutritional intervention studies usually produce mild transcriptional effects and in many cases, no genes pass FDR selection (17). Therefore, we consider the BC-induced changes in *Fzd6* and *Cthrc1* gene expression as being important and further focused on these two genes, especially because these two genes may be involved in the same pathway. The expression of the genes *Fzd6* and *Cthrc1* was compared between all four groups; control *Bcmo1*$^{+/+}$, BC-supplemented *Bcmo1*$^{+/+}$, control *Bcmo1*$^{-/-}$ and BC-supplemented *Bcmo1*$^{+/+}$ to examine if effects were specific for BC supplementation in *Bcmo1*$^{-/-}$ mice. Indeed, BC supplementation resulted in a significant downregulation of *Fzd6* and *Cthrc1* only in *Bcmo1*$^{-/-}$ mice and not in *Bcmo1*$^{+/+}$ mice (Figure 3C).

Overrepresented GO processes by BC supplementation in Bcmo1$^{-/-}$

SOM analysis is a technique that groups genes with a similar interindividual gene expression pattern in the same cluster. The distance between the clusters in the clustering profile represents the degree of difference in gene expression patterns (18). We applied SOM analysis to identify genes regulated with similar interindividual variations in gene expression as *Fzd6* and *Cthrc1*. The total number of SOM profiles was set to 144, corresponding to an average of ∼10 genes per profile (12). SOM analysis clustered all genes into only five clusters from the 144 possible clusters. Moreover, clusters were relatively close together, which indicates that all regulated genes ($P < 0.05$) have a relatively similar variation in gene expression pattern between animals (Figure 4).

Knowledge is limited concerning the function of *Cthrc1* and *Fzd6* in lung. Overrepresented GO processes might result in a hypothesis concerning the function of BC or BC-induced *Fzd6* and *Cthrc1* regulation in lung tissue. Since significantly regulated genes had a relative similar gene expression pattern according to SOM analysis, we performed GO using the bioinformatics tool ErmineJ, using all genes and their corresponding *P*-values, and not a subset of genes. The four overrepresented GO processes with the lowest *P*-value were as follows: GO:0007608, sensory perception of smell ($P = 1.89 \times 10^{-9}$); GO:0007606, sensory perception of chemical stimulus ($P = 1.54 \times 10^{-8}$) and GO:0007156, homophilic cell adhesion ($P = 2.44 \times 10^{-08}$) (supplementary Table III is available at *Carcinogenesis* Online). The GO processes sensory perception of smell and sensory perception of chemical stimulus contained the same different *olfactory receptors* (*Olfr*) (26 different *Olfr* and *Cyclic nucleotide-gated channel alpha 2* (*Cnga2*) $P < 0.05$) (Table II). The GO process homophilic cell adhesion contained mainly different forms of the clustered cadherin family (nine different *Protocadherin beta's*, two *Protocadherins*, two different *Cadherins* and *Desmoglein* $P < 0.05$) (Table II). Q-PCR confirmed the upregulation of *Olfr437* and *Pcdhb9* in *Bcmo1*$^{-/-}$ mice after BC supplementation (Figure 5A and B). The significantly regulated *Olfr* and *Protocadherins* were present in all SOM profiles, which had relatively similar average gene expression patterns between the animals.

Discussion

In this study, we assessed effects of BC supplementation in male wild-type (*Bcmo1*$^{+/+}$) mice, which are able to metabolize BC to a high extent, and in male *Bcmo1*-knockout (*Bcmo1*$^{-/-}$) mice, which are unable to symmetrically cleave BC. Indeed, the concentration of BC in serum and lung was increased to a higher level in *Bcmo1*$^{-/-}$ mice than in *Bcmo1*$^{+/+}$ mice after BC supplementation. Genome-wide transcriptome analysis revealed that around two times more genes were regulated in *Bcmo1*$^{-/-}$ mice than in *Bcmo1*$^{+/+}$ mice by BC supplementation. BC supplementation in *Bcmo1*$^{-/-}$ mice resulted in three main, very significant findings. First, the genes *Fzd6* and *Cthrc1* were both very significantly downregulated (FDR < 0.05) with a fold change of −2.99 and −2.60, respectively. These genes are both involved in the Wnt–Fzd pathway that is important in the regulation of cell fate determination and development. Second, many olfactory receptors and members of the clustered protocadherin family were upregulated, and the presence of both groups of genes is mainly reported in neuronal cells. A third observation was that the interindividual gene expression patterns between the genes were highly similar. Pulmonary neuroendocrine cells (PNECs) are highly associated with sensory nerves and are involved in stem cell

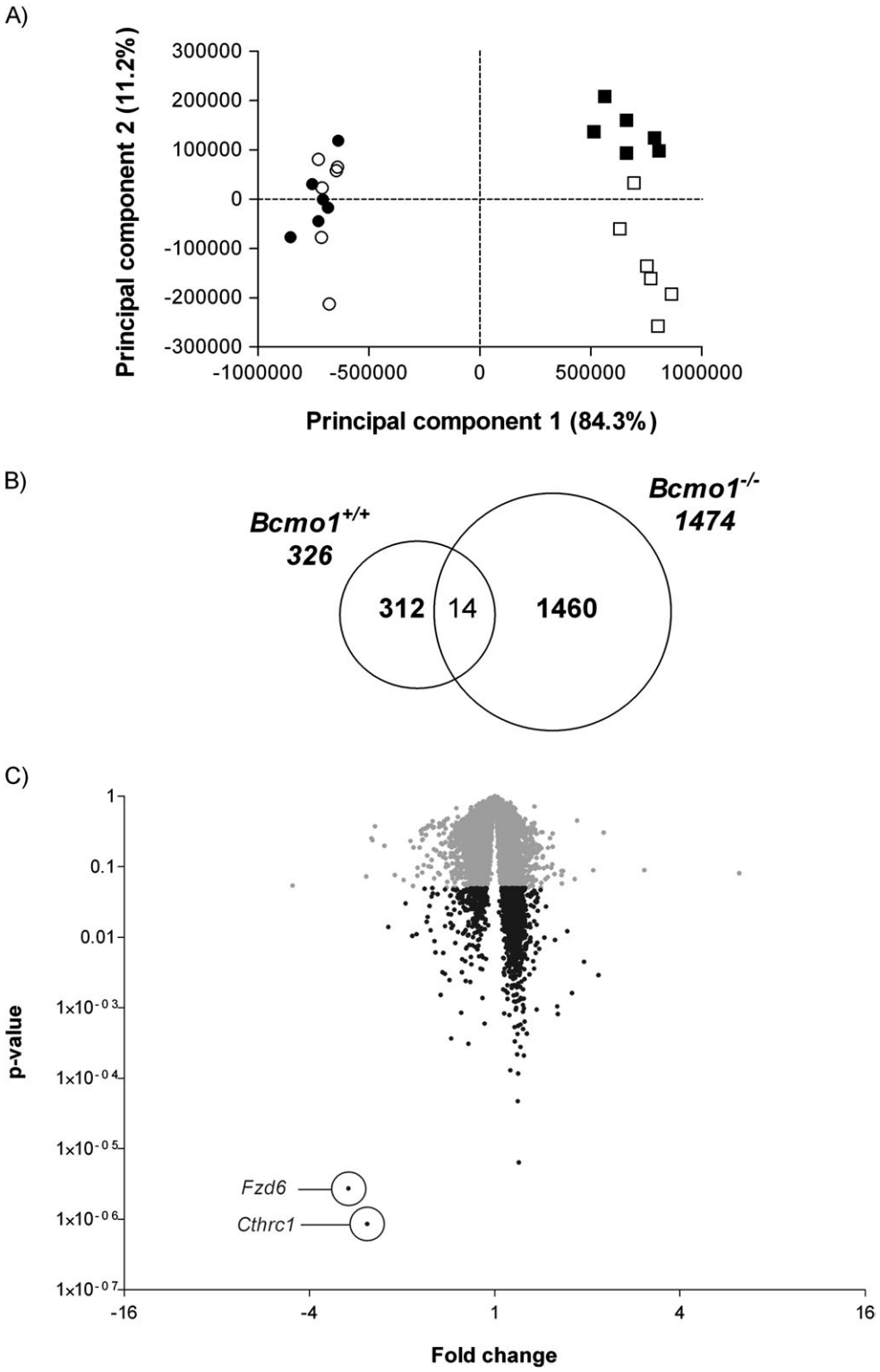

Fig. 2. Presentation of BC-induced gene expression effects in *Bcmo1*$^{+/+}$ and *Bcmo1*$^{-/-}$ mice. (**A**) Supervised principal component analysis of *Bcmo1*$^{+/+}$ mice (circles), *Bcmo1*$^{-/-}$ (squares) receiving a control diet (open symbol) or BC diet (closed symbol). Mice are clearly separated based on genotype (*x*-axis) and *Bcmo1*$^{-/-}$ mice receiving the BC diet are clearly separated from *Bcmo1*$^{-/-}$ control mice. (**B**) Venn diagram representing the number of regulated genes ($P < 0.05$) upon BC supplementation in *Bcmo1*$^{+/+}$ mice (left circle) and *Bcmo1*$^{-/-}$ mice (right circle) and the number of overlapping regulated genes in both groups. (**C**) Volcano plot representing the effect of BC supplementation on fold change gene expression difference in *Bcmo1*$^{-/-}$ mice compared with the control diet (*x*-axis) and the corresponding Student's *t*-test *P*-value on the *y*-axis. This plot clearly shows a similar low *P*-value and relatively high absolute fold change for both *Cthrc1* and *Fzd6*. In gray, are all genes with $P > 0.05$ and in black, all genes with $P < 0.05$.

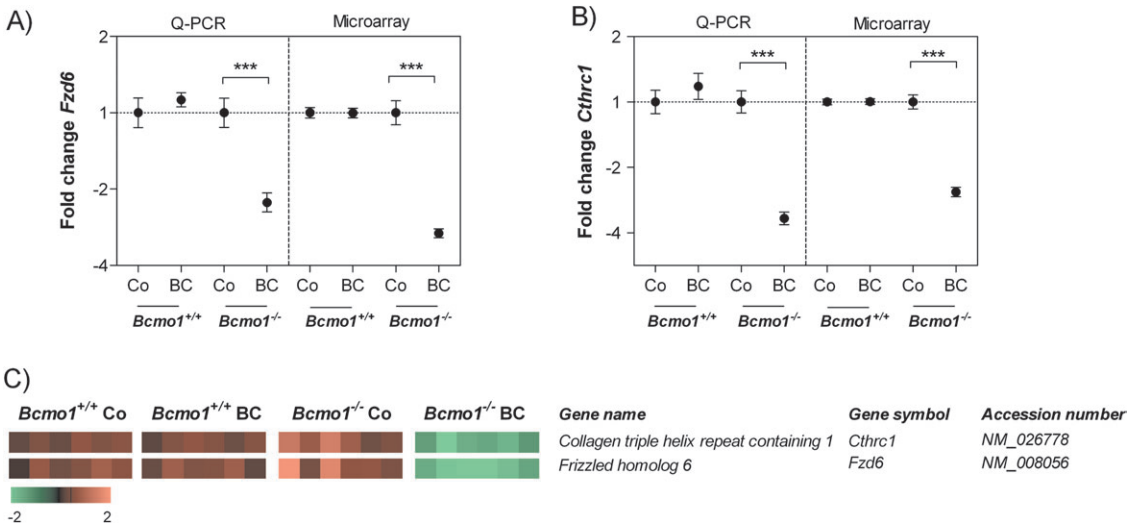

Fig. 3. Gene expression of *Fzd6* and *Cthrc1*. The expression of the genes *Fzd6* (**A**) and *Cthrc1* (**B**) in the BC-supplemented mice relative to the control diet-fed mice were confirmed by Q-PCR using the stable reference genes *Stx5a* and *Rnf130*. Data represent the average gene expression ± SEM compared with $Bcmo1^{+/+}$ control mice. $^{***}P < 0.001$ using a Student's *t*-test on the log-transformed data. (**C**) Microarray-based heatmap shows a low interindividual difference between the mice for the genes *Cthrc1* and *Fzd6* and a decreased gene expression of these genes in BC-supplemented $Bcmo1^{-/-}$ mice compared with $Bcmo1^{+/+}$ mice and $Bcmo1^{-/-}$ control mice.

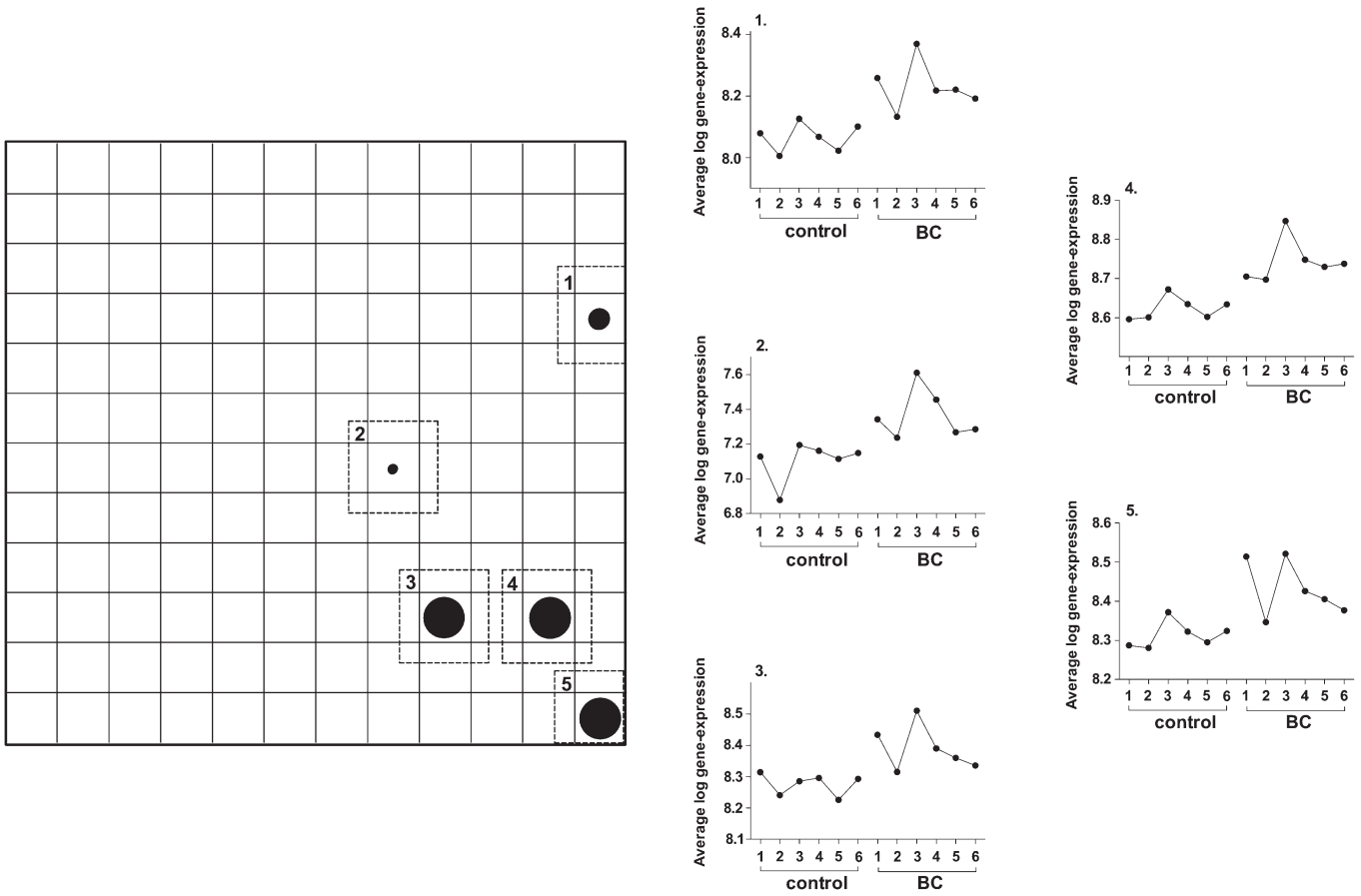

Fig. 4. SOM analysis of genes regulated by BC in $Bcmo1^{-/-}$ mice ($P < 0.05$). SOM profile for BC-regulated genes ($P < 0.05$) in $Bcmo1^{-/-}$ mice. SOM analysis presents all genes with a similar interindividual gene expression within one group. The number of possible SOM profiles was set to 144, corresponding to an average of ~10 genes per profile (12). The average gene expression pattern of every cluster is plotted with corresponding cluster numbers. Average log gene expression (*y*-axis) per cluster is plotted per animal (*x*-axis) with a rank of increasing animal number per group.

development during injury and repair. Since the BC-regulated genes are involved in neuronal and developmental pathways, BC might specifically affect the highly innervated PNECs. A role for BC in the regulation of PNECs might be of particular importance in smoke-induced lung carcinogenesis since PNEC tumors comprise ~20% of all lung cancers and are strongly associated with tobacco use.

Table II. Genes present ($P < 0.05$) in the three most significantly BC-regulated GO processes as determined by ErmineJ in lung tissue of *Bcmo1*$^{-/-}$ mice

Gene symbol	Gene name	Sequence ID	Probe name	Gene expression[a]		Gene expression[b]	
				Bcmo1$^{+/+}$ Co	*Bcmo1*$^{+/+}$ BC	*Bcmo1*$^{-/-}$ Co	*Bcmo1*$^{+/+}$ BC
GO:0007608 sensory perception of smell and GO:0007606 sensory perception of chemical stimulus[c]							
Olfr945	*olfactory receptor 945*	NM_146506	A_51_P200249	1.00	1.15 (n.s.)	1.00	1.21 (0.004)
Cnga2	*cyclic nucleotide gated channel alpha 2*	NM_007724	A_51_P423948	1.00	1.05 (n.s.)	1.00	1.16 (0.006)
Olfr437	*olfactory receptor 437*	NM_146296	A_51_P108555	1.00	1.03 (n.s.)	1.00	1.23 (0.011)
Olfr1131	*olfactory receptor 1131*	NM_146658	A_51_P113058	1.00	1.00 (n.s.)	1.00	1.11 (0.012)
Olfr570	*olfactory receptor 570*	NM_147110	A_51_P352864	1.00	1.05 (n.s.)	1.00	1.14 (0.013)
Olfr411	*olfactory receptor 411*	NM_146709	A_51_P191572	1.00	1.01 (n.s.)	1.00	1.17 (0.013)
Olfr1417	*olfactory receptor 1417*	NM_146936	A_51_P115139	1.00	−1.02 (n.s.)	1.00	1.18 (0.014)
Olfr126	*olfactory receptor 126*	NM_146890	A_51_P149531	1.00	1.03 (n.s.)	1.00	1.23 (0.016)
Olfr973	*olfactory receptor 973*	NM_146613	A_52_P415047	1.00	1.09 (n.s.)	1.00	1.10 (0.020)
Olfr197	*olfactory receptor 197*	NM_146484	A_52_P133333	1.00	−1.01 (n.s.)	1.00	1.19 (0.021)
Olfr74	*olfactory receptor 74*	NM_054091	A_51_P123314	1.00	1.04 (n.s.)	1.00	1.14 (0.024)
Olfr569	*olfactory receptor 569*	NM_147088	A_51_P347206	1.00	−1.02 (n.s.)	1.00	1.12 (0.027)
Olfr1342	*olfactory receptor 1342*	NM_146713	A_51_P373583	1.00	1.07 (n.s.)	1.00	1.15 (0.033)
Olfr159	*olfactory receptor 159*	NM_019476	A_51_P112682	1.00	1.04 (n.s.)	1.00	1.09 (0.034)
Olfr611	*olfactory receptor 611*	NM_146727	A_51_P129972	1.00	1.08 (n.s.)	1.00	1.13 (0.034)
Olfr446	*olfactory receptor 446*	NM_146295	A_51_P514902	1.00	1.05 (n.s.)	1.00	1.16 (0.037)
Olfr1411	*olfactory receptor 1411*	NM_146490	A_51_P275365	1.00	−1.05 (n.s.)	1.00	1.17 (0.039)
Olfr1030	*olfactory receptor 1030*	NM_146588	A_51_P276149	1.00	1.03 (n.s.)	1.00	1.13 (0.041)
Olfr870	*olfactory receptor 870*	NM_146904	A_51_P201751	1.00	−1.00 (n.s.)	1.00	1.11 (0.042)
Olfr668	*olfactory receptor 668*	NM_147059	A_51_P515949	1.00	1.03 (n.s.)	1.00	1.09 (0.042)
Olfr397	*olfactory receptor 397*	NM_146346	A_51_P352636	1.00	1.04 (n.s.)	1.00	1.14 (0.043)
Olfr266	*olfactory receptor 266*	NM_146489	A_52_P358720	1.00	−1.02 (n.s.)	1.00	1.08 (0.044)
Olfr187	*olfactory receptor 187*	NM_146322	A_51_P386280	1.00	−1.01 (n.s.)	1.00	1.16 (0.045)
Olfr469	*olfactory receptor 469*	NM_146426	A_52_P313007	1.00	1.08 (n.s.)	1.00	1.10 (0.046)
Olfr239	*olfactory receptor 239*	NM_207175	A_51_P484279	1.00	1.12 (n.s.)	1.00	1.20 (0.047)
Olfr1419	*olfactory receptor 1419*	NM_001011775	A_52_P232438	1.00	1.07 (n.s.)	1.00	1.16 (0.047)
Olfr740	*olfactory receptor 740*	NM_146667	A_52_P390844	1.00	1.04 (n.s.)	1.00	1.14 (0.049)
GO:0007156: Homophilic cell adhesion							
Pcdhb16	*protocadherin beta 16*	NM_053141	A_51_P191743	1.00	−1.00 (n.s.)	1.00	1.24 (0.000)
Pcdhb9	*protocadherin beta 9*	NM_053134	A_51_P483878	1.00	−1.12 (n.s.)	1.00	1.23 (0.007)
Pcdh12	*protocadherin 12*	NM_017378	A_52_P515769	1.00	1.01 (n.s.)	1.00	1.26 (0.007)
Pcdhb7	*protocadherin beta 7*	NM_053132	A_51_P184223	1.00	1.12 (n.s.)	1.00	1.40 (0.007)
Pcdhb18	*protocadherin beta 18*	NM_053143	A_51_P511918	1.00	1.05 (n.s.)	1.00	1.15 (0.011)
Pcdhb4	*protocadherin beta 4*	NM_053129	A_52_P529195	1.00	−1.09 (n.s.)	1.00	1.72 (0.012)
Pcdhb15	*protocadherin beta 15*	NM_053140	A_51_P159833	1.00	1.02 (n.s.)	1.00	1.20 (0.014)
Celsr2	*cadherin EGF LAG seven-pass G-type receptor 2*	NM_017392	A_52_P350148	1.00	1.10 (n.s.)	1.00	1.12 (0.015)
Pcdhb5	*protocadherin beta 5*	NM_053130	A_51_P257292	1.00	−1.03 (n.s.)	1.00	1.11 (0.017)
Cdh22	*cadherin 22*	NM_174988	A_51_P373573	1.00	1.09 (n.s.)	1.00	1.18 (0.022)
Pcdh1	*protocadherin 1*	NM_029357	A_51_P239257	1.00	−1.03 (n.s.)	1.00	−1.13 (0.030)
Dsg2	*desmoglein 2*	NM_007883	A_52_P88091	1.00	1.03 (n.s.)	1.00	1.14 (0.031)
Pcdhb6	*protocadherin beta 6*	NM_053131	A_51_P403413	1.00	−1.01 (n.s.)	1.00	1.10 (0.033)
Pcdhb10	*protocadherin beta 10*	NM_053135	A_51_P289066	1.00	−1.05 (n.s.)	1.00	1.13 (0.035)

n.s., non-significant difference ($P > 0.05$) between BC-supplemented *Bcmo1*$^{+/+}$ mice and control *Bcmo1*$^{+/+}$ mice.
[a]Gene expression relative to average gene expression in *Bcmo1*$^{+/+}$ control mice (*P*-value).
[b]Gene expression relative to average gene expression in *Bcmo1*$^{-/-}$ control mice (*P*-value).
[c]Both GO processes contain the same genes.

In this study, we found a notable downregulation of *Fzd6* and *Cthrc1* by dietary BC in *Bcmo1*$^{-/-}$ mice. *Fzd6* encodes a member of the Frizzled receptor family of transmembrane receptors for Wnt signals (19) and *Cthrc1* encodes a secreted protein (20). Both *Fzd6* and *Cthrc1* were downregulated to a similar degree and had a similar FDR suggesting that these genes were jointly regulated. This is in line with recent findings that *Cthrc1* stabilizes the Wnt–Fzd complex (21). The main known function of *Fzd6* that emerges among the relatively limited number of studies on this protein is its involvement in patterning during development (22). But the precise functions of *Fzd6* and *Cthrc1* are, as yet, unknown for the lung. *Fzd6* might have an important function in the lung since it is highly expressed in adult and fetal human lung tissue (23).

The highly significant BC-induced downregulation of *Fzd6* and *Cthrc1* was observed in combination with an upregulation of many different olfactory receptors, protocadherins and cadherins in the *Bcmo1*$^{-/-}$ mice. Clustered protocadherins are highly expressed in neurons and become highly enriched at synapses during development, and their expression decreases after neuronal maturation (24). The main described function of olfactory receptors is that they bind odorant molecules in the olfactory bulb to result in a neuronal signal transduction through sensory nerves. Although the name 'olfactory receptor' implicates a function only in olfaction, the presence and a function for olfactory receptors in tissues other than the olfactory bulb, has been described (25,26). The function for olfactory receptors in the lung is unknown, but it is tempting to speculate that they might have a role in sensing the environment. In line with this, similar as in olfaction, sensory neurons are important in the lung to allow the lung to detect differences in the environment. The main function of sensory neurons in the lung is to allow the lung to react to differences in air composition, such as reduced oxygen tension (hypoxia) (27,28) or differences in CO_2 concentrations (29,30). A possible function for olfactory receptors in the lung might thus be the detection of changes in the air composition.

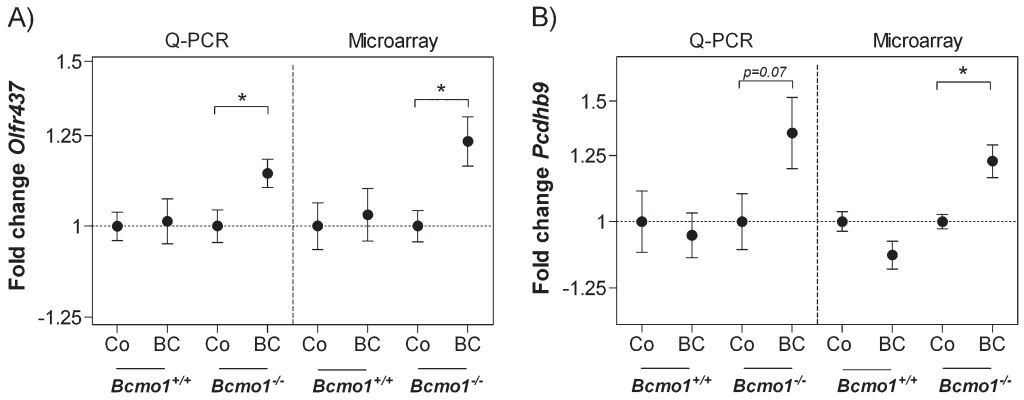

Fig. 5. Validation of microarray results. The expression of the genes *Olfr437* (**A**) and *Pcdhb9* (**B**) in BC-supplemented mice relative to control diet-fed mice analyzed by microarray analysis and Q-PCR using the stable reference genes S*tx5a* and *Rnf130*. Data represent the average gene expression ± SEM compared with control diet-fed mice. $^{*}P < 0.05$ using a Student's *t*-test on the log-transformed data.

There is one cell type present in lung tissue that is highly associated and innervated with sensory nerves (28,31,32) and that has the ability to react to changes in air composition. These cells are the PNECs and it has been described that PNECs are able to detect for example hypoxia by the use of receptors that are highly similar to olfactory receptors (27,28). PNECs can be present as solitary cells or as clusters called the neuroepithelial bodies (33). Besides a role for the highly innervated PNECs in airway chemoreception, it has been shown that the neuroepithelial body microenvironment is highly important for lung stem cell development during injury and repair (34–36). Wnt signaling has been proposed to be key regulator in stem cell control and development (37). This dual function for the innervated PNECs in both chemodetection and in control of development are in correspondence with our findings: regulation of *Fzd6*, *Cthrc1* and regulation of olfactory receptors and protocadherins. However, we cannot conclude that there is a general increase or decrease in the number of PNECs since *Fzd6* and *Cthrc1* were downregulated, whereas the olfactory receptors and the protocadherins were mainly upregulated. We can speculate on this. It is known that sensory nerves involved in olfaction are generated and regenerated from neuronal stem cells every 40 days throughout a lifetime (38), but the generation and regeneration of sensory nerves is, as far as we know, unknown for the lung. Generation and regeneration of sensory nerves might also be important in the lung and therefore, it is tempting to assume that there might be an important function of the stem cell developmental genes *Fzd6* and *Cthrc1* in sensory neurogenesis, resulting in an upregulation of olfactory receptors and protocadeherins. The Wnt–Fzd complex can activate the canonical pathway for cell differentiation or alternatively, signals the non-canonical pathway for control of cell movement and tissue polarity (39,40). The non-canonical pathway can be further subdivided into the wnt/Ca^{2+} pathway, which is not very well characterized at this moment, and into the wnt/planar cell polarity pathway that is typically involved in hair patterning and cell motility by the control of actin polymerization (41). Although *Cthrc1* and *Fzd6* are both implicated in the wnt/planar cell polarity process and the main known function of *Fzd6* is the control of developmental patterning, *Fzd6* was also found to suppress the canonical pathway in *Fzd6*-transfected cells (21). Indeed, in lung epithelial cells, an increase in confluence resulted in an increase in *Fzd6* and a decrease in activation of the canonical pathway (42). Our findings in BC-supplemented animals show the same mechanism but in the opposite direction; a downregulation of *Fzd6* in combination with an upregulation of olfactory receptors, protocadherins and cadherins (supplementary Figure 1 is available at *Carcinogenesis* Online).

The next question is whether our data might explain —part of— the mechanism underlying the increased lung cancer risk upon BC supplementation in smokers (ATBC and CARET). Small-cell lung carcinoma and the most significant form of large-cell lung carcinoma, large-cell neuroendocrine lung carcinoma, originate both from PNECs (43,44). In total, PNECs are present in lung very sparsely with a frequency of 1 PNEC per 2500 epithelial cells (45) however, PNEC-derived tumors account for ∼20% of all lung cancers and is highly associated with tobacco use (46). In the CARET study, the risk for large-cell lung carcinoma was significantly increased due to BC supplementation (4). The control of stem cells is important to avoid undesired cell growth, which ultimately can result in cancer (47). The Wnt pathway is one of the most important pathways involved in stem cell control and a dysregulation of these genes can result in uncontrolled growth of lung cancer cells (48,49) and might be one of the explanations in the involvement of BC in the increased lung cancer risk in smokers of the ATBC and CARET study.

In our study, BC supplementation to *Bcmo1*$^{-/-}$ mice resulted in a downregulation of *Fzd6* and *Cthrc1* in combination with an increase in the neuronal olfactory receptors and in members of the protocadherin family. BC itself was never associated with neuronal cell development, although its downstream metabolite, retinoic acid is. Retinoic acid is a ligand for the RARs and the RXRs. Depletion of vitamin A, a precursor for retinoic acid, or the knockout of the RAR and/or RXR receptor results in defects of the nervous system (50), implicating that retinoic acid is of importance in neurogenesis. Moreover, aldehyde dehydrogenase 1 family, member a3 (Aldh1a3), an important and rate-limiting enzyme in the synthesis of retinoic acid, has been shown to be present at high concentrations in the neuroepithelium and is therefore an important neuroepithelial marker. Mice without a functional *Aldh1a3* enzyme show morphological defects in the nasal cavity, the most important site of the generation of olfactory neurons (51). As can be seen in Table I, we showed that several enzymes important in downstream BC metabolism were changed in *Bcmo1*$^{-/-}$ mice compared with *Bcmo1*$^{+/+}$ mice. Although BC was especially high in the *Bcmo1*$^{-/-}$ mice and BC metabolite concentrations were especially high in the *Bcmo1*$^{+/+}$ mice it is unknown at this moment whether high BC concentrations or for example alterations in the availability of retinoic acid caused the effects as we have described here for BC supplementation in male *Bcmo1*$^{-/-}$ mice.

Altogether we demonstrated that BC was able to accumulate in lungs of *Bcmo1*$^{-/-}$ mice, thereby decreasing *Fzd6* and *Cthrc1* gene expression with a fold change of −2.99 and −2.60, respectively. Moreover, many olfactory receptors and many members of the protocadherin family were upregulated. The interindividual differences in gene expression of the significantly ($P < 0.05$) regulated genes was low and therefore resulted in a high correlation of the expression of the genes as analyzed by SOM analysis. A specific role for the highly expressed *Fzd6* gene and *Cthrc1* in lung tissue has never been described. We hypothesize that BC decreases the regulation of both *Fzd6* and *Cthrc1*, which possibly have a joint function and that by the downregulation of these two genes, olfactory receptors and protocadherins are increased. These processes might be of importance in smoke- or asbestos-induced lung carcinogenesis and are possibly affected by BC.

Supplementary material

Supplementary Figure 1 and Tables I–III can be found at http://carcin.oxfordjournals.org/

Funding

Y.v.H. is funded by NUTRIM/VLAG.

Acknowledgements

J.K. is a member of Mitofood (COST FA0602). We thank DSM neutraceuticals for the use of *Bcmo1*$^{-/-}$ mice and the BC beadlets and the European Nutrigenomics Organization (Network of Excellence, EU Contract FOOD-CT-2004-506360) for support of the animal study.

Conflict of Interest Statement: None declared.

References

1. van Poppel,G. (1996) Epidemiological evidence for beta-carotene in prevention of cancer and cardiovascular disease. *Eur. J. Clin. Nutr.*, **50** (suppl. 3), S57–S61.
2. Ziegler,R.G. (1989) A review of epidemiologic evidence that carotenoids reduce the risk of cancer. *J. Nutr.*, **119**, 116–122.
3. Albanes,D. *et al*. (1996) Alpha-Tocopherol and beta-carotene supplements and lung cancer incidence in the alpha-tocopherol, beta-carotene cancer prevention study: effects of base-line characteristics and study compliance. *J. Natl Cancer Inst.*, **88**, 1560–1570.
4. Omenn,G.S. *et al*. (1996) Risk factors for lung cancer and for intervention effects in CARET, the Beta-Carotene and Retinol Efficacy Trial. *J. Natl Cancer Inst.*, **88**, 1550–1559.
5. Hennekens,C.H. *et al*. (1996) Lack of effect of long-term supplementation with beta carotene on the incidence of malignant neoplasms and cardiovascular disease. *N. Engl. J. Med.*, **334**, 1145–1149.
6. Palozza,P. (1998) Prooxidant actions of carotenoids in biologic systems. *Nutr. Rev.*, **56**, 257–265.
7. van Helden,Y.G. *et al*. (2009) Beta-carotene metabolites enhance inflammation-induced oxidative DNA damage in lung epithelial cells. *Free Radic. Biol. Med.*, **46**, 299–304.
8. Russell,R.M. (2004) The enigma of beta-carotene in carcinogenesis: what can be learned from animal studies. *J. Nutr.*, **134**, 262S–268S.
9. von Lintig,J. *et al*. (2000) Filling the gap in vitamin A research. Molecular identification of an enzyme cleaving beta-carotene to retinal. *J. Biol. Chem.*, **275**, 11915–11920.
10. von Lintig,J. *et al*. (2001) Molecular analysis of vitamin A formation: cloning and characterization of beta-carotene 15,15'-dioxygenases. *Arch. Biochem. Biophys.*, **385**, 47–52.
11. Hessel,S. *et al*. (2007) CMO1 deficiency abolishes vitamin A production from beta-carotene and alters lipid metabolism in mice. *J. Biol. Chem.*, **282**, 33553–33561.
12. Rodenburg,W. *et al*. (2008) A framework to identify physiological responses in microarray-based gene expression studies: selection and interpretation of biologically relevant genes. *Physiol. Genomics*, **33**, 78–90.
13. van Schothorst,E.M. *et al*. (2007) Assessment of reducing RNA input for Agilent oligo microarrays. *Anal. Biochem.*, **363**, 315–317.
14. Wettenhall,J.M. *et al*. (2004) limmaGUI: a graphical user interface for linear modeling of microarray data. *Bioinformatics*, **20**, 3705–3706.
15. Pellis,L. *et al*. (2003) The intraclass correlation coefficient applied for evaluation of data correction, labeling methods, and rectal biopsy sampling in DNA microarray experiments. *Physiol. Genomics*, **16**, 99–106.
16. Lee,H.K. *et al*. (2005) ErmineJ: tool for functional analysis of gene expression data sets. *BMC Bioinformatics*, **6**, 269.
17. Keijer,J. *et al*. (2009) Transcriptome analysis in benefit-risk assessment of micronutrients and bioactive food components. *Mol. Nutr. Food Res.*, **54**, 240–248.
18. Tamayo,P. *et al*. (1999) Interpreting patterns of gene expression with self-organizing maps: methods and application to hematopoietic differentiation. *Proc. Natl Acad. Sci. USA*, **96**, 2907–2912.
19. Bhanot,P. *et al*. (1996) A new member of the frizzled family from Drosophila functions as a Wingless receptor. *Nature*, **382**, 225–230.
20. Pyagay,P. *et al*. (2005) Collagen triple helix repeat containing 1, a novel secreted protein in injured and diseased arteries, inhibits collagen expression and promotes cell migration. *Circ. Res.*, **96**, 261–268.
21. Yamamoto,S. *et al*. (2008) Cthrc1 selectively activates the planar cell polarity pathway of Wnt signaling by stabilizing the Wnt-receptor complex. *Dev. Cell*, **15**, 23–36.
22. Guo,N. *et al*. (2004) Frizzled6 controls hair patterning in mice. *Proc. Natl Acad. Sci. USA*, **101**, 9277–9281.
23. Tokuhara,M. *et al*. (1998) Molecular cloning of human Frizzled-6. *Biochem. Biophys. Res. Commun.*, **243**, 622–627.
24. Morishita,H. *et al*. (2007) Protocadherin family: diversity, structure, and function. *Curr. Opin. Cell Biol.*, **19**, 584–592.
25. Weber,M. *et al*. (2002) Olfactory receptor expressed in ganglia of the autonomic nervous system. *J. Neurosci. Res.*, **68**, 176–184.
26. Yagi,T. (2008) Clustered protocadherin family. *Dev. Growth Differ.*, **50** (suppl. 1), S131–S40.
27. Adriaensen,D. *et al*. (2003) Functional morphology of pulmonary neuroepithelial bodies: extremely complex airway receptors. *Anat. Rec. A Discov. Mol. Cell Evol. Biol.*, **270**, 25–40.
28. Linnoila,R.I. (2006) Functional facets of the pulmonary neuroendocrine system. *Lab. Invest.*, **86**, 425–444.
29. Hu,J. *et al*. (2007) Detection of near-atmospheric concentrations of CO2 by an olfactory subsystem in the mouse. *Science*, **317**, 953–957.
30. Lahiri,S. *et al*. (2003) CO2/H(+) sensing: peripheral and central chemoreception. *Int. J. Biochem. Cell Biol.*, **35**, 1413–1435.
31. Pan,J. *et al*. (2004) Innervation of pulmonary neuroendocrine cells and neuroepithelial bodies in developing rabbit lung. *J. Histochem. Cytochem.*, **52**, 379–389.
32. Weichselbaum,M. *et al*. (2005) A confocal microscopic study of solitary pulmonary neuroendocrine cells in human airway epithelium. *Respir. Res.*, **6**, 115.
33. Van Lommel,A. *et al*. (1999) The pulmonary neuroendocrine system: the past decade. *Arch. Histol. Cytol.*, **62**, 1–16.
34. De Proost,I. *et al*. (2009) Purinergic signaling in the pulmonary neuroepithelial body microenvironment unraveled by live cell imaging. *FASEB J.*, **23**, 1153–1160.
35. Peake,J.L. *et al*. (2000) Alteration of pulmonary neuroendocrine cells during epithelial repair of naphthalene-induced airway injury. *Am. J. Pathol.*, **156**, 279–286.
36. Reynolds,S.D. *et al*. (2000) Neuroepithelial bodies of pulmonary airways serve as a reservoir of progenitor cells capable of epithelial regeneration. *Am. J. Pathol.*, **156**, 269–278.
37. Michaelidis,T.M. *et al*. (2008) Wnt signaling and neural stem cells: caught in the Wnt web. *Cell Tissue Res.*, **331**, 193–210.
38. Beites,C.L. *et al*. (2005) Identification and molecular regulation of neural stem cells in the olfactory epithelium. *Exp. Cell Res.*, **306**, 309–316.
39. Katoh,M. *et al*. (2007) WNT signaling pathway and stem cell signaling network. *Clin. Cancer Res.*, **13**, 4042–4045.
40. Golan,T. *et al*. (2004) The human Frizzled 6 (HFz6) acts as a negative regulator of the canonical Wnt. beta-catenin signaling cascade. *J. Biol. Chem.*, **279**, 14879–14888.
41. Devenport,D. *et al*. (2008) Planar polarization in embryonic epidermis orchestrates global asymmetric morphogenesis of hair follicles. *Nat. Cell Biol.*, **10**, 1257–1268.
42. Steel,M.D. *et al*. (2005) Beta-catenin/T-cell factor-mediated transcription is modulated by cell density in human bronchial epithelial cells. *Int. J. Biochem. Cell Biol.*, **37**, 1281–1295.
43. Fernandez,F.G. *et al*. (2006) Large-cell neuroendocrine carcinoma of the lung. *Cancer Control*, **13**, 270–275.
44. Travis,W.D. *et al*. (1995) Lung cancer. *Cancer*, **75**, 191–202.
45. Gosney,J.R. *et al*. (1988) Neuroendocrine cell populations in normal human lungs: a quantitative study. *Thorax*, **43**, 878–882.
46. Gustafsson,B.I. *et al*. (2008) Bronchopulmonary neuroendocrine tumors. *Cancer*, **113**, 5–21.
47. Reya,T. *et al*. (2005) Wnt signalling in stem cells and cancer. *Nature*, **434**, 843–850.
48. Kim,J. *et al*. (2007) Wnt inhibitory factor inhibits lung cancer cell growth. *J. Thorac. Cardiovasc. Surg.*, **133**, 733–737.
49. You,L. *et al*. (2004) Inhibition of Wnt-2-mediated signaling induces programmed cell death in non-small-cell lung cancer cells. *Oncogene*, **23**, 6170–6174.
50. Dickman,E.D. *et al*. (1997) Temporally-regulated retinoic acid depletion produces specific neural crest, ocular and nervous system defects. *Development*, **124**, 3111–3121.
51. Dupe,V. *et al*. (2003) A newborn lethal defect due to inactivation of retinaldehyde dehydrogenase type 3 is prevented by maternal retinoic acid treatment. *Proc. Natl Acad. Sci. USA*, **100**, 14036–14041.

Received December 17, 2009; revised April 5, 2010; accepted April 10, 2010